Reverse Startup Procedure for Multi Terminal Smart Transformer Supplying Data Centres

Anandh N
Graduate Student Member, IEEE
Dept. of EEE, IIT Guwahati
Guwahati, India
Dept. of EEE, MIT Manipal
Manipal Academy of Higher Education
Manipal, India
anandh_n@iitg.ac.in

Dwijasish Das
Member, IEEE
Dept. of ESE, TU Delft
Delft, Netherlands
d.das-1@tudelft.nl

Chandan Kumar
Senior Member, IEEE
Dept. of EEE, IIT Guwahati
Guwahati, India
chandank@iitg.ac.in

2025 IEEE Guwahati Subsection Conference (GCON) | 979-8-3315-1345-0/25/$31.00 ©2025 IEEE | DOI: 10.1109/GCON65540.2025.11173345

***Abstract*—A reverse startup procedure for a multi terminal smart transformer (MTST) supplying data centres, transitioning from islanded operation to grid connected operation is proposed in this paper. During islanded operation, the MTST low voltage (LV) converter remains active, while the MTST multi active bridge (MAB) converter is partially active and MTST medium voltage (MV) converter is inactive. To facilitate reconnection to the MV grid from the LV side, these converters need to be activated to allow the power flow. In this operation, the power is drawn from a battery energy storage system (BESS) connected to LVdc_1 bus to charge the MTST MVdc bus. Once the MVdc bus is sufficiently charged, the MTST-MV converter is initiated to establish the connection between the LV side and the MV grid. Simulation is performed in PSCAD and the results are provided to validate the effectiveness of this startup operation.**

***Index Terms*—Battery energy storage system (BESS), data centres, islanding, LVdc loads, multi terminal smart transformer (MTST).**

I. Introduction

The architecture of recent information/communication technology (ICT) infrastructures, such as data centres, is being restructured to seamlessly integrate with traditional grid, incorporate DC sources like renewable energy sources (RES)/battery energy storage systems (BESS), and efficiently supply power to both AC and DC loads [1], [2]. The AC and DC sources/loads integrates to form a hybrid power architecture is an ideal choice for data centres [3].

Solid state transformer (SST), facilitates the hybrid architecture of data centres by enabling interaction with the AC utility grid. SSTs providing key capabilities including bidirectional power flow management and harmonic mitigation, enhances power quality and the integration of RES/BESS [4], [5]. The data centres are substantial loads in the power system, they are typically connected to medium voltage ac (MVac) grids. Consequently, MVac to low voltage dc (MVac-LVdc) conversion is essential for data centre operations, making SSTs a financially viable alternative to traditional low frequency transformer (LFT) solutions [6], [7]. A concept for a multi terminal smart transformer (MTST) tailored for use in green data centres is presented in [8]. This system employs multi active bridge (MAB) converter for dc to dc stage and is capable of delivering quality power in both ac/dc forms across different voltage levels as required. Furthermore, its ac/dc terminals offer the flexibility to connect RES/BESS.

A startup strategy is proposed for a three stage SST [9], with the objective of reducing high frequency transformer (HFT) currents during startup. This strategy coordinates the startup of ac/dc and dc-dc converter in a regulated fashion, equalizing the primary/secondary voltages of the transformer. A new soft start procedure tailored for ST incorporating cascaded H bridge and dual active bridge converters, controlled as a unified converter is presented in [10]. Initially, during startup, CHB converter functions as rectifier and the dc to dc stage gradually modify the voltages of dc link capacitors to desired level. The modulation technique with DAB converters enables the limitation of inrush currents, preventing overcurrent and overshoots. The startup/restart schemes of 3-stage modular SSTs is examined in [11]. To mitigate inrush currents during SST start-up, a control strategy for DAB with an extended delay time is utilized. A partial-startup scheme for three stage ST was proposed for a meshed-hybrid islanded grid is discussed in [12]. This startup procedure ensures the smooth activation of MV converter and isolated dc-dc converter, facilitating the connection of LVdc side to MVac grid without disrupting the ST-LV converter's operation.

This paper presents a reverse startup procedure for MTST, enabling reconnection to MV grid from LV edge islanded operation. The paper is arranged as follows. Section II describes the system and Section III explains the operating principle of MAB converter. The description for the reverse startup operation is elaborated in Section IV, and in Section V, the control strategies of the MTST is discussed. Section VI provides the simulation results, and in Section VII, the conclusion is drawn.

This publication is supported by IIT Guwahati Technology Innovation and Development Foundation (TIDF) under project grant TIH/TD/0407 and in part by the Science and Engineering Research Board (SERB), Department of Science and Technology, India, under the Research Grant CRG/2022/001685.

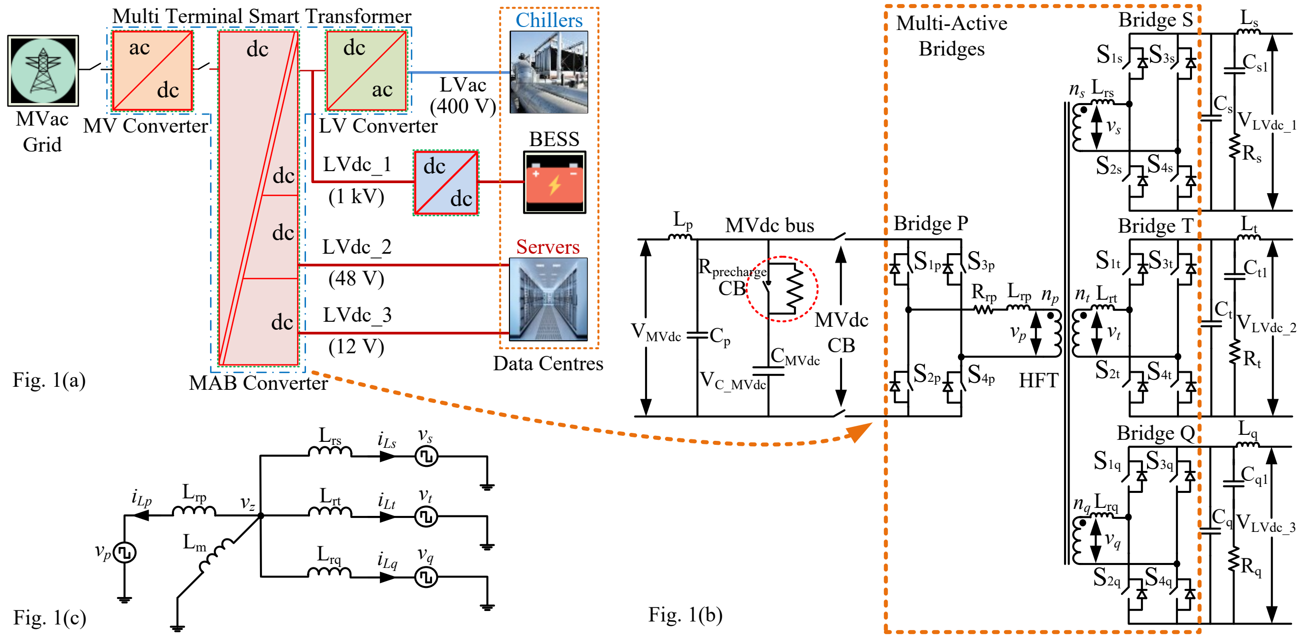

Fig. 1. (a) Schematic of MTST fed data centres. (b) Topology of MAB converter. (c) Y equivalent model of MAB converter.

II. System Description

A BESS integrated MTST feeding data centres is depicted in Fig. 1(a). The power transfer between MV grid and LVac/LVdc loads takes place via MTST-MV converter, MAB converter, and LV converter. During grid connected operation, the BESS interfaced with LVdc_1 bus operates in current controlled mode (CCM) enables charging or discharging. During islanding operation, the MTST-MV converter is inactive and MAB converter operates as triple-active bridge (TAB) converter. Whenever the MVdc bus is switched off, LVdc_1 bridge takes over as primary, correspondingly the LVdc_2 and LVdc_3 bridges acts as secondary and tertiary, respectively. The BESS maintains LVdc_1 bus voltage, ensuring continuous power to LV loads. The MTST-LV converter regulates LVac voltage/frequency.

III. Operating Principle of MAB Converter

A MAB converter consists of n full bridge modules linked via n winding HFT with magnetic coupling. In this work, an asymmetrical quadruple-active bridge (AQAB) converter is considered comprising of four active bridges labeled as P, S, T, and Q for analysis purpose and its topology is shown in Fig. 1(b). Each bridge's elements are marked with subscripts (p, s, t, q) indicating their respective bridge. For analyzing the MAB converter's operation and switching conditions, a Y equivalent model shown in Fig. 1(c) is utilized. In this model, the bridges are substituted with rectangular voltage sources and denoted as v_p, v_s, v_t and v_q. The midpoint voltage v_z and the inductor's current slope are calculated as follows, where $x \in (p, s, t, q)$.

$$v_z = \frac{v_p + v_s + v_t + v_q}{4}. \tag{1}$$

$$\frac{di_{Lx}}{dt} = \frac{v_x - v_z}{L_w} \tag{2}$$

where, $$L_w = L_{rp} = L_{rs} = L_{rt} = L_{rq}. \tag{3}$$

If all LV side parameters are referred to the MV side, the LV side inductances and voltages are expressed as follows:

$$L'_{rs} = \left(\frac{n_p}{n_s}\right)^2 L_{rs}, L'_{rt} = \left(\frac{n_p}{n_t}\right)^2 L_{rt}, L'_{rq} = \left(\frac{n_p}{n_q}\right)^2 L_{rq}. \tag{4}$$

$$V'_{LVdc\_1} = \left(\frac{n_p}{n_s}\right) V_{LVdc\_1}, ...V'_{LVdc\_n} = \left(\frac{n_p}{n_n}\right) V_{LVdc\_n}. \tag{5}$$

The converter employs phase-shift modulation (PSM) to regulate power. This technique involves applying rectangular voltages (v_p, v_s, v_t and v_q) to the transformer with varying phase shifts (ϕ_p, ϕ_s, ϕ_t, and ϕ_q) and a constant switching frequency (f_s). By adjusting the phase difference between the bridges, power control is achieved. For an MAB converter with n bridges, the power equation used to calculate the individual power transfer between each bridge is given by

$$P_{ml} = \frac{V_m V_l}{2\pi \ f_s L_{ml}} \phi_{ml} \left(1 - \frac{|\phi_{ml}|}{\pi}\right) \tag{6}$$

$$\phi_{ml} = \phi_m - \phi_l \tag{7}$$

where V_m and V_l are bridge dc voltages, ϕ_m and ϕ_l - angles of phase shift, f_s - switching frequency, L_{ml} - inductance equivalence of bridges m and l.

IV. Description of Reverse Startup Operation

The startup procedure facilitates the reconnection of LVac side to MVac side via MTST. The reverse startup process undergoes three modes of operation namely, initial precharging

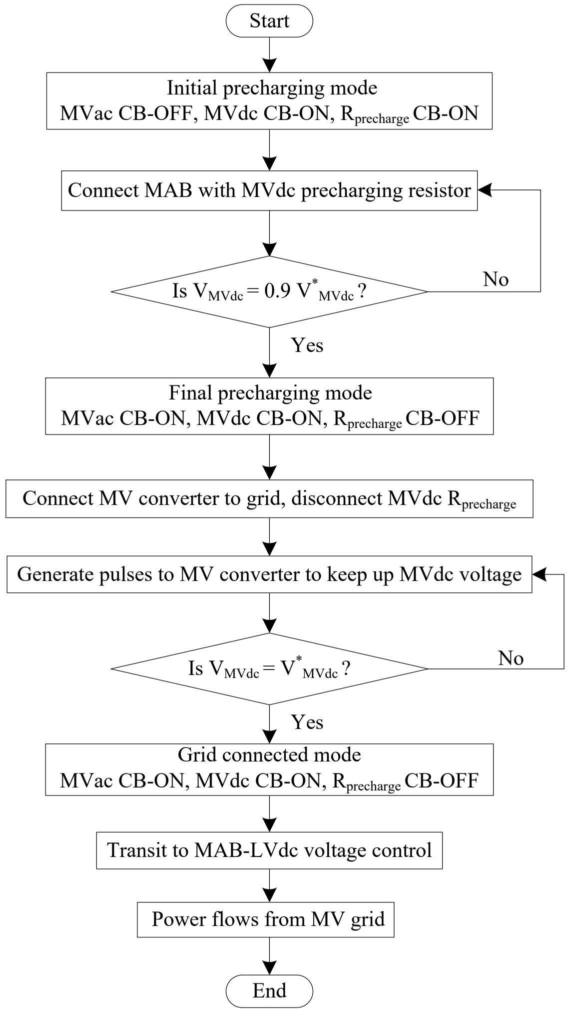

Fig. 2. Flowchart for the reverse startup operation.

mode, final precharging mode and grid connecting mode. Initial precharging mode deals with the operation of MAB converter; final precharging mode involves the MV converter in action; and grid connected mode establishes the reconnection of LVac side to MVac grid. The flow chart for the reverse startup scheme is depicted in Fig. 2. Further elaboration on each mode follows.

A. Initial precharging mode

This mode charges the MVdc bus to 0.9 times of its reference voltage. This is facilitated by the MTST-MAB converter, which draws power from LVdc_1 to the MVdc bus. To reduce the initial starting current, a series resistor is employed alongside MVdc capacitor for voltage rampup, as illustrated in Fig. 1(b). After reaching the nominal voltage level, the precharging resistor is cut off. If P_{MAB}^{max} denotes the maximum power of MAB, then the precharging resistor's value is calculated as

$$R_{MVdc}^{precharge} = \frac{\left[(\frac{n_1}{n_n})V_{LVdc\_n}\right]^2}{P_{MAB}^{max}} \tag{8}$$

where $(\frac{n_1}{n_n})$ represents the transformer turns ratio and V_{LVdc_n} denotes the LVdc voltages for n arms of the MAB. Therefore, when the MAB is connected to the LV side, the MVdc capacitor will charge from the LV side without the need for any phase-shift. This leads to a sudden inrush of capacitor charging current. To reduce this current, a precharging resistor is used. When MVdc voltage attains 90% of its reference value, the pulses to MAB are switched off, and precharging resistor is disconnected.

The time constant of the MVdc capacitor precharging circuit is given by

$$\tau = R_{MVdc}^{precharge} \times C_{MVdc}. \tag{9}$$

During the capacitor charging phase, the voltage of the MVdc capacitor, V_{C_MVdc} is determined by capacitor charging equation and can be expressed as:

$$V_{C\_MVdc} = V_{MVdc}\left\{1 - e^{\left(-\frac{t}{R_{MVdc}^{precharge} \times C_{MVdc}}\right)}\right\} \tag{10}$$

where t represents the time duration and C_{MVdc} denotes the capacitance of MVdc link.

Considering, 90% of reference MVdc voltage for the MVdc capacitor, (10) can be written as

$$1 - e^{\left(-\frac{t}{R_{MVdc}^{precharge} \times C_{MVdc}}\right)} = 0.9. \tag{11}$$

(11) can be simplified to:

$$t = 2.302 \times R_{MVdc}^{precharge} \times C_{MVdc}. \tag{12}$$

The minimum value of $R_{MVdc}^{precharge}$ is determined using (8), while (12) is utilized to estimate the timespan for precharging the MVdc link capacitor.

B. Final precharging mode

In this mode, the MTST-MV converter is activated to charge MVdc bridge to its specified desired voltage. A control mechanism is employed to offset switch losses, ensuring that power is extracted from MV edge to charge MVdc bridge to the specified voltage level. The power consumed by MTST-MV converter is solely utilized for charging the MVdc bus. To prevent excessive current draw, a hard limit is imposed on reference currents generated for MTST-MV converter, ensuring that the peak current remains within the converter's rated capacity. This reduces startup current stress on MTST-MV converter.

C. Grid connected mode

The BESS converter switches to CCM, and the MTST-MAB converter regulates the LV side voltages facilitating the system's transition to grid connected operation. The power delivered from the BESS is capped at a fixed level. Consequently, any excess power demand on the LV edge is met by drawing power from MV grid through the MTST-MV and MAB converters, facilitating the system's changeover to grid-connected mode.

V. Control Strategies

This section outlines the control strategies for each converter in the system. Fig. 3 presents the control strategies of MTST.

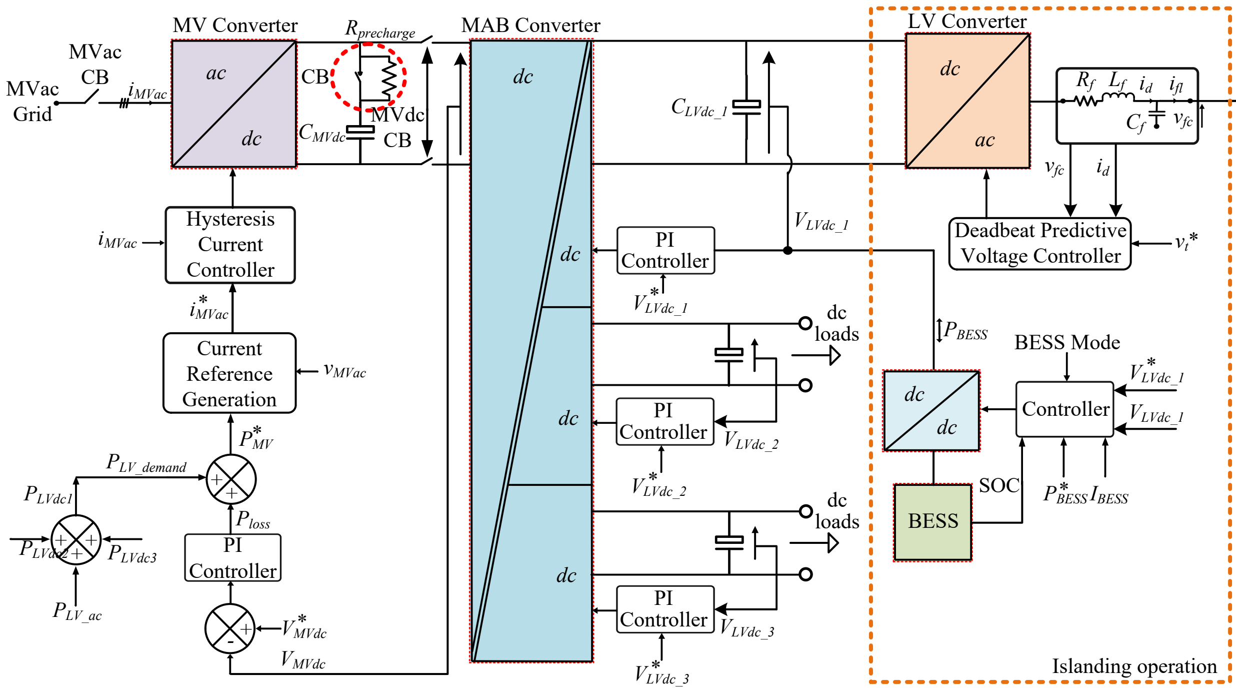

Fig. 3. Control diagram of MTST.

A. MTST-MV converter

This converter consumes total required power, including system losses, from MVac grid. A PI controller is employed to estimate system losses. By incorporating these losses into total power demand, the MVdc voltage is regulated. The equation can be seen below:

$$P_{loss} = K_{ploss} e_{MVdc} + K_{iloss} \int e_{MVdc} dt \tag{13}$$

where e_{MVdc} - actual and reference MVdc voltage error, K_{ploss} - proportional gain constant and K_{iloss} - integral gain constant.

The total power consumed by MTST-MV converter is given by the following expression:

$$P^*_{MV} = P_{loss} + P_{LV\_demand}. \tag{14}$$

During startup procedure, the MTST-MV converter is solely responsible for charging MVdc bridge, and hence the component P_{LV_demand} is not included in P^*_{MV}. As a result, P^*_{MV} consists only of P_{loss}. Upon successful reconnection to the MVac grid, the P_{LV_demand} is incorporated into the overall power of MTST-MV converter. This is utilized as reference power to produce reference currents. Hysteresis current control is employed to align actual MVac currents with their reference values.

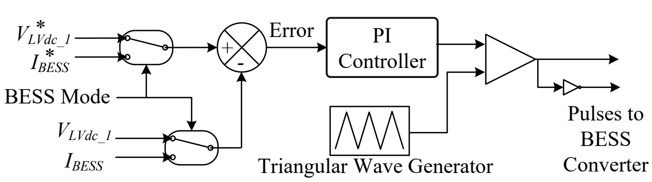

Fig. 4. BESS Controller.

TABLE I
SIMULATION PARAMETERS

System quantities	Values
MVac voltage	11 kV (L-L)
LVac voltage	0.4 kV (L-L)
MTST-MV converter	S_{rated} = 100 kVA, L_{fm} = 100 mH, C_{fm} = 1 μF, C_{MVdc} = 1350 μF
MTST-MAB converter	S_{rated} = 100 kVA, No. of windings = 4, f_s = 2 kHz, V_{MVdc} = 20 kV, V_{LVdc_1} = 1 kV, V_{LVdc_2} = 48 V, V_{LVdc_3} = 12 V
MTST-LV converter	S_{rated} = 100 kVA, C_{LVdc} = 4700 μF, L_f = 1 mH, C_f = 20 μF
BESS dc-dc converter	P_{rated} = 1.5 MW, f_s = 10 kHz, L = 1 mH, C = 100 μF

B. MTST-MAB converter

The control is achieved by varying phase delay between primary and secondary bridge firing sequences. The primary side operates with a pulse having a 50% duty cycle. On secondary side, multi-windings feed power to respective bridge of MAB. A multi-terminal transformer is employed, with winding ratios determined based on needed voltage levels. This relationship is written as follows:

$$n_p : n_s : n_t : n_q = V_{MVdc} : V_{LVdc\_1} : V_{LVdc\_2} : V_{LVdc\_3}. \tag{15}$$

The delay in the firing sequence for each bridge is calculated based on its output voltage reference in relation to the primary side. This is achieved using a Proportional-Integral (PI) controller.

C. MTST-LV converter

This converter manages voltage/frequency on LVac edge during both island/grid connected operations. The reference voltage is maintained at 230 V/phase and 50 Hz. The deadbeat

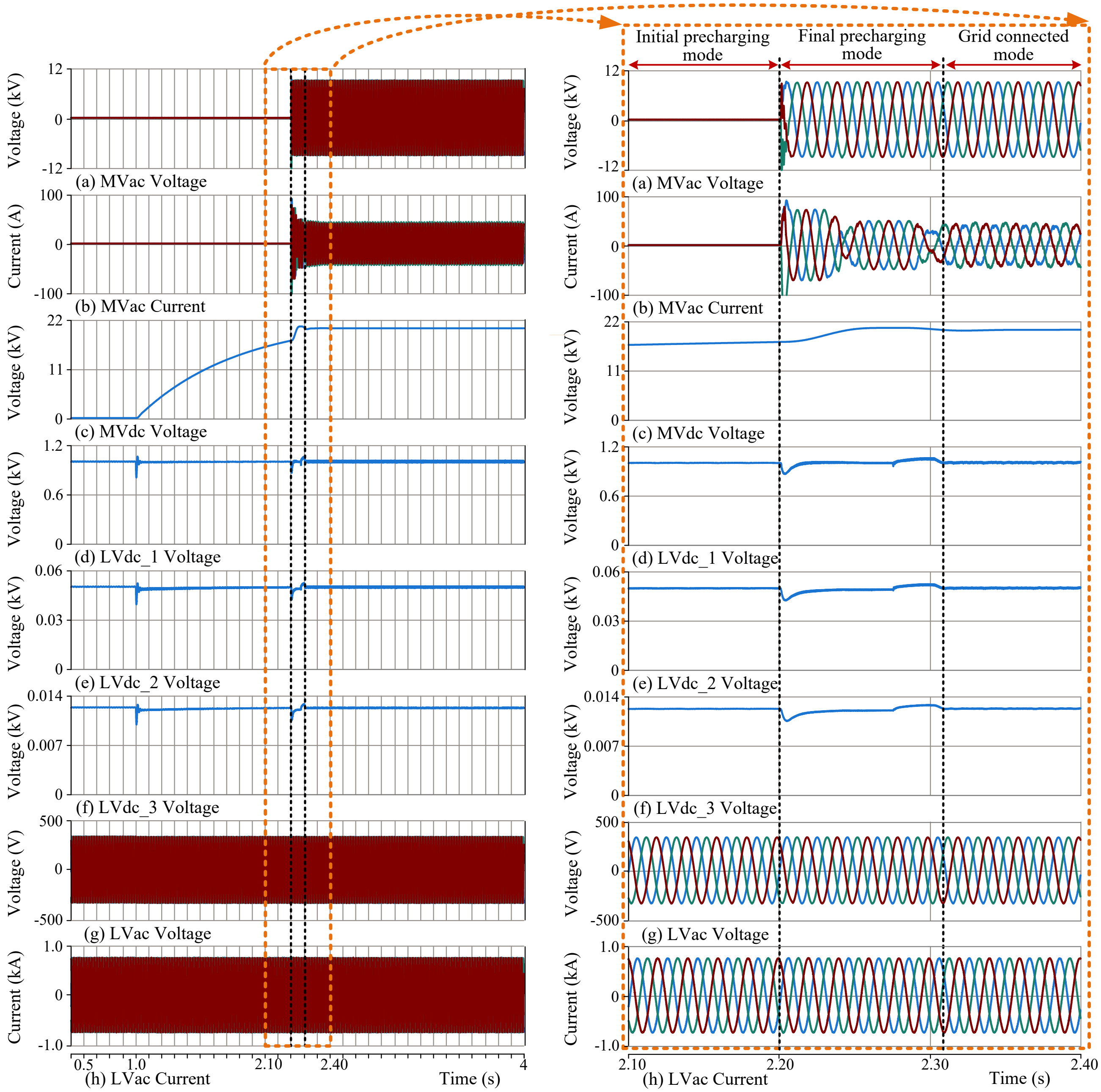

Fig. 5. (i) Transition of voltage and current waveforms stage by stage during reverse startup operation. (a) MVac voltage. (b) MVac current. (c) MVdc voltage. (d) LVdc_1 voltage. (e) LVdc_2 voltage. (f) LVdc_3 voltage. (g) LVac voltage. (h) LVac current. (ii) Zoomed view of voltage and current waveforms.

control scheme is employed to ensure precise regulation of the LVac voltage.

D. BESS dc-dc converter

During grid connection, BESS converter works in CCM. However, while operating in UPS mode, it shifts to VCM to ensure a stable LVdc_1 bus voltage. In VCM, the controller continuously tracks LVdc_1 and compares it with reference voltage. A PI controller is used to adjust the actual voltage with respect to reference voltage, ensuring stability. Based on the PI controller output, pulses are generated to control the converter operation effectively. The controller for BESS is depicted in Fig. 4.

VI. Simulation Results

The system is modeled and simulated using PSCAD. The simulation parameters are provided in Table I. Initially, the system operates in islanded mode, with the BESS regulating LVdc_1 voltage and MTST-LV converter controlling the LVac voltage. The system voltages/currents are illustrated in Fig. 5(i) and Fig. 5(ii). At t = 1 s, the reconnecting process commences by closing the MVdc CB. The MVdc voltage gradually rises

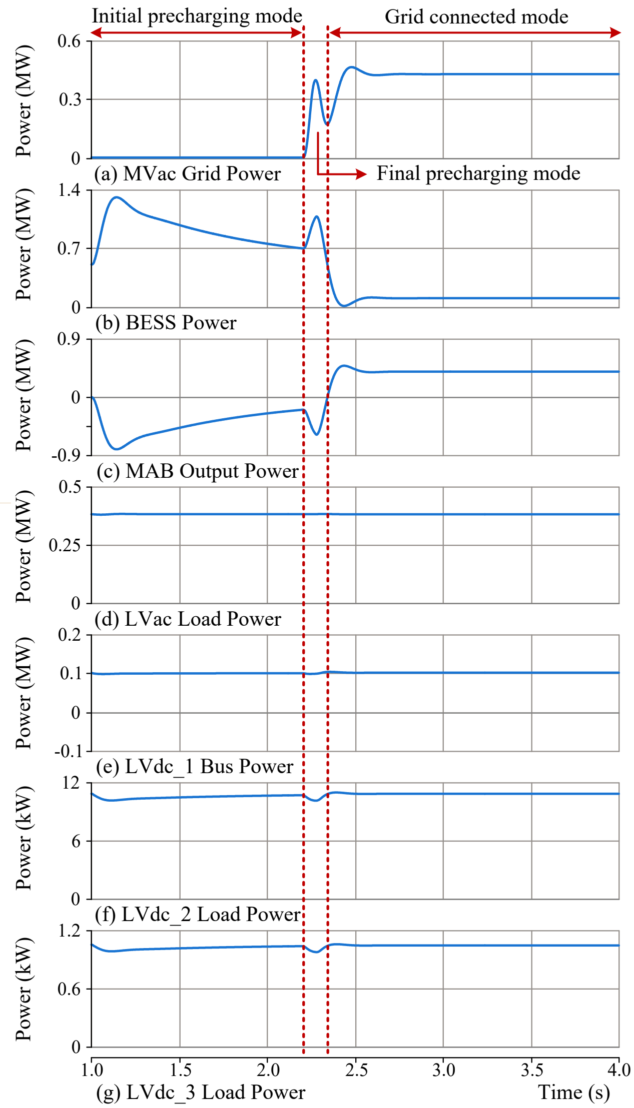

Fig. 6. Active power flows in the system. (a) MVac grid power. (b) BESS power. (c) MAB output power. (d) LVac load power. (e) LVdc_1 bus power. (f) LVdc_2 load power. (g) LVdc_3 load power.

until it reaches 0.9 times the reference MVdc voltage. Upon reaching this voltage level on MVdc edge, the second mode initiates, and then the MTST-MV converter receives switching pulses to rise the MVdc voltage to its reference value of 20 kV. Once this voltage threshold is attained, the regulation of LVdc voltages is transferred to the MTST-MAB converter and the BESS transits to CCM, enabling the system to operate in grid connecting mode.

The LVac load takes power from BESS via MTST-LV converter. Fig. 6 illustrates the active power flows in the system. The LVac load consumes a constant power of 0.4 MW, while LVdc_1 bus consumes 0.1 MW consistently during the starting phase. The LVdc_2 and LVdc_3 loads draw power of 10 kW and 1 kW, respectively. The BESS starts feeding power once MVdc capacitor begins charging. BESS power increases initially and then decreases as capacitor charging current reduces. Concurrently, MTST-MAB converter absorbs this power, resulting in negative power flow. When MVdc voltage hits 90% of its reference value, the MTST-MV converter draws power from grid. Upon completion of startup process, the powers stabilize to steady values confirming the effectiveness of reverse startup scheme.

VII. Conclusion

This paper proposes a reverse startup method for a MTST supplying data centres transitioning from island to grid connected operation. In this process, the BESS charges MVdc bus by enabling power flow from LVdc_1 bus through MAB converter. To restrict excessive current draw, a current limit resistor is utilized during the charging process, ensuring the MVdc bus charges within safe current and power limits. At last, MTST-MV converter is engaged to establish grid connected operation.

References

[1] Rothmund, Daniel and Guillod, Thomas and Bortis, Dominik and Kolar, Johann W., “99% Efficient 10 kV SiC-Based 7 kV/400 V DC Transformer for Future Data Centers,” *IEEE J. Emerg. Sel. Topics Power Electron.*, vol. 7, no. 2, pp. 753-767, 2019.

[2] Loh, Poh Chiang and Li, Ding and Chai, Yi Kang and Blaabjerg, Frede, “Hybrid ACDC Microgrids With Energy Storages and Progressive Energy Flow Tuning,” *IEEE Trans. Power Electron.*, vol. 28, no. 4, pp. 1533-1543, 2013.

[3] Shrestha, Bijen R. and Tamrakar, Ujjwol and Hansen, Timothy M. and Bhattarai, Bishnu P. and James, Sean and Tonkoski, Reinaldo, “Efficiency and Reliability Analyses of AC and 380 V DC Distribution in Data Centers,” *IEEE Access*, vol. 6, pp. 63305-63315, 2018.

[4] Huber, Jonas E. and Kolar, Johann W., “Applicability of Solid-State Transformers in Todays and Future Distribution Grids,” *IEEE Trans. Smart Grid*, vol. 10, no. 1, pp. 317-326, 2019.

[5] She, Xu and Huang, Alex Q. and Burgos, Rolando, “Review of Solid-State Transformer Technologies and Their Application in Power Distribution Systems,” *IEEE J. Emerg. Sel. Topics Power Electron.*, vol. 1, no. 3, pp. 186-198, 2013.

[6] Sidorov, Andrey and Zinoviev, Gennady and Petzoldt, Jrgen, “Solid State Transformer as a Part Electrical Circuit for Data Center Application,” *IEEE 22nd Int. Conf. Young Professionals in Electron Devices and Mater. (EDM)*, 2021, pp. 354-359.

[7] Agrawal, Alok and Nalamati, Chandra Sekhar and Gupta, Rajesh, “Hybrid DCAC Zonal Microgrid Enabled by Solid-State Transformer and Centralized ESD Integration,” *IEEE Trans. Ind. Electron.*, vol. 66, no. 11, pp. 9097-9107, 2019.

[8] Das, Dwijasish and N, Anandh and Kumar, Chandan, “Multi-Terminal Smart Transformer for Green Data Centres,” *IEEE 13th Int. Symp. Power Electron. Distrib. Gener. Syst.*, (PEDG), 2022, pp. 1-6.

[9] Liu, Xiaohu and Li, Hui and Wang, Zhan, “A Start-Up Scheme for a Three-Stage Solid-State Transformer With Minimized Transformer Current Response,” *IEEE Trans. Power Electron.*, vol. 27, no. 12, pp. 4832-4836, 2012.

[10] Pugliese, Sante and Buticchi, Giampaolo and Mastromauro, Rosa Anna and Andresen, Markus and Liserre, Marco and Stasi, Silvio, “Soft-Start Procedure for a Three-Stage Smart Transformer Based on Dual-Active Bridge and Cascaded H-Bridge Converters,” *IEEE Trans. Power Electron.*, vol. 35, no. 10, pp. 11039-11052, 2020.

[11] Zhang, Xueyin and Xu, Yonghai and Siddique, Abubakar and Long, Yunbo and Xiao, Xiangning, “A Microprocessor Resource-Saving Dual Active Bridge Control for Startup and Restart of Three-Stage Modular Solid-State Transformer,” *IEEE Trans. Power Del.*, vol. 35, no. 3, pp. 1443-1454, 2020.

[12] Das, Dwijasish and Kumar, Chandan, “Partial Startup Scheme for Smart Transformer in Meshed Hybrid Islanded Grid Operation,” *IEEE Trans. Ind Appl.*, vol. 58, no. 1, pp. 142-151, 2022.